Textures and Microstructures, 1991, Vols 14–18, pp. 1067–1072
Reprints available from the publisher
Photocopying permitted by license only

DEFORMATION TEXTURE AND MICROSTRUCTURE OF A CROSS ROLLED {112}<111> CRYSTAL OF Cu 5wt% Al

G.D. Köhlhoff*, Hsun Hu** and K. Lücke***
* Thyssen Edelstahlwerke AG, Magnetfabrik Dortmund, Ostkirchstr.177, D-4600 Dortmund 41, FRG
** Department of Materials Science and Engineering, University of Pittsburgh, Pittsburgh PA 15261, USA
*** Institut für Metallkunde und Metallphysik, RWTH Aachen, Kopernikusstr.14, D-5100 Aachen, FRG

INTRODUCTION

Texture development during straight rolling of polycrystalline fcc metals with low stacking fault energy has been investigated for many decades. It was found that twinning of the {112}<111> component and the subsequent rotation of the matrix-twin packages toward {111}<112> followed by shear band formation are essential features for the formation of the "brass-type" rolling texture [1]. With respect to the theory of such texture formation, however, many questions remain open and several models are under discussion.

The present work was designed to give detailed information on the deformation behaviour of the {112}<111> component by investigating single crystal behaviour. Furthermore, cross rolling was applied to test the mechanical twinning and deformation faulting mechanism for the "brass-type" texture formation.

EXPERIMENTAL PROCEDURE

Material

Cu 5wt% Al {112}<111> single crystals (10x25x120mm^3) were grown by a Bridgeman technique using high purity copper (99.995%) and aluminium (99.998%).

Rolling

Cross rolling to various reductions from 50% to 95% was carried out on a rolling mill (roll diameter = 250mm) by changing the rolling direction (RD) clockwise after each step by 90° about the normal direction (ND). Rolling reductions were chosen to give constant strain of approximately 2%. The accuracy of the rolling mill adjustment of 0.01mm, however, did not allow an adjustment of the rolling gap to obtain a true constant strain, especially at higher rolling reductions. In these cases several reduction steps were carried out at constant rolling gap settings.

Investigation of texture and microstructure

X-ray diffraction pole figures were measured in the midthickness plane of the specimens and three-dimensional orientation distribution function (ODF) analysis [2] was applied for quantitative evaluation. Microstructure development was observed by transmission electron microscopy (TEM) on specimens cut from longitudinal and transverse sections, i.e. sections perpendicular to RD_2 and RD_1, respectively.

RESULTS

Texture

(111) pole figures of the as-grown crystal and cross rolled specimens after 50%, 70%, 80%, 90%, and 95% reductions are shown in Figure 1. The corresponding ODFs for the deformed state have been determined, but are not shown. The skeleton lines along the τ- and α-fibre, respectively, taken from ODFs are shown in Figure 2. The τ-fibre runs in the $\varphi_2=45°$ cut at $\varphi_1=90°$ from $\Phi=0°$ to $\Phi=90°$. It corresponds to an orientation rotation about TD, which is RD_2 in the case of cross rolling. The α-fibre representing an orientation rotation about ND is also located in the $\varphi_2=45°$ cut and runs at $\Phi=90°$ from $\varphi_1=90°$to $\varphi_1=0°$.

Up to 50% reduction (Figures 1b and 2) the texture development is dominated by {552}<115> twin formation about that (111) pole of the initial orientation (Figure 1a) which lies closest to ND. At this stage the intensity f(g) of the twin is about 4.5 times as high as the intensity of the matrix orientation. In addition a low intensity shows up on the α-fibre 10° away from {011}<100>. With increasing reduction twin formation is followed by a cooperative rotation of the matrix-twin components about RD_2. This leads at 70% (Figures 1c and 2) into {111}<112>. The intensity of the orientation within 10° {011}<100> increases at the same time. After 80% reduction (Figures 1d and 2) the {111}<112> intensity decreased and the ND smeared {011}-<100> intensity increases. By additional rolling to 90% and 95% (Figures 1e,f and 2) the {111}<112> component is further reduced and the {011}<100> component reaches its maximum after 90%. The orientation rotation from 90% to 95% is dominated by a rotation about ±ND (α-fibre) out of the {011}<100> component. The texture after 95% reduction consists of an orientation tube running from {011}<100> toward {011}<211> with an intensity maximum which lies about 18° away from the ideal {011}<211> (brass) component.

Microstructure

The microstructure is shown for the 80% rolled specimen in Figure 3. In the longitudinal section the matrix-twin lamellae are approximately aligned parallel to RD_1 and cut by shear bands. Newly formed bands form angles of about +35° and -40° to RD_1. The well developed shear band lies at about -23° to RD_1.

DISCUSSION

Texture development during cross rolling up to 95% of the {112}<111> Cu 5%wt Al crystal (Figures 1 and 2) shows an unexpected simple orientation path. It essentially leads towards the {110}<112> "brass-type" texture which is formed in

straight rolled polycrystals [3] and also {112}<111>-oriented single crystals of fcc metals with low stacking fault energy (SFE) [4]. It might be expected that in cross rolling a more complicated texture develops, since with alternating rolling directions (RD_1 and RD_2) two different orientations {112}<111> and {112}<110>, respectively, contribute to deformation. From earlier work in copper rolled at RT {112}<111> [5] is known to be a stable orientation whereas {112}<110> is unstable. It splits up into two symmetrical orientations, which are near {123}<634>[6]. For low SFE materials, only results on {112}<111> are available and these show that it twins [4]. The onset of twinning was determined in copper rolled at 77 K to occur already at 10% reduction [5]. The similarities in texture development of straight and cross rolled {112}<111> low SFE metals suggest that texture formation in the present case is controlled by the rolling in RD_1.

To explain the orientation path considerations on the active slip systems must be done by analysis of the possible normal and partial slip systems operating in the respective orientations. This is done by calculating the Schmid factors μ_n and μ_p, respectively, on the basis of a biaxial stress system which is an approximation to strip or sheet rolling. The resolved shear stress is thus given by

$$\tau = \sigma (\cos\Phi_t \cos\lambda_t + \cos\Phi_c \cos\lambda_c)$$

where σ is the applied stress, Φ_t and λ_t are the angles subtended by the slip plane normed and the slip direction, respectively with the tension axis (the RD); and Φ_c and λ_c are similar angles made by the same slip elements with reference to the compression axis (the rolling plane normal). The available slip systems with respect to RD_1 and RD_2 are shown in the stereographic projections in Figure 4. (111) slip plane normals are labeled A-D; <110> and <112> slip directions are indicated by roman and arabic numbers, respectively.

For the {112}<111> orientation, i.e. during RD_1 rolling the systems AV, AVI, BI and DI have the highest Schmid factor for normal slip (μ_n=0.54) and A3 is the most favourable partial slip system (μ_p=0.63). Due to the high μ_p/μ_n ratio of 1.15 the partial slip system A3 is the prefered operated one and twinning and deformation faulting is to occur already at low reductions. What, however, is striking is the high volume fraction of {552}<115> twin orientation of about 80%. The matrix-twin ratio in straight rolled {112}<111> Cu 4wt% Al or copper at 77 K is about 1 [4,5].

With respect to RD_2 ({112}<110>) the slip systems BII, DIII and B9, D6 are those with the highest Schmid factors μ_n=0.81 and μ_p=0.79, respectively. At μ_p/μ_n=0.96 which is considerably lower than in RD_1 twinning is more difficult and should occur only at higher reductions. Thus at the beginning of rolling normal slip is the dominant deformation mode and orientation splitting should eventually occur, as it does in straight rolled {112}<110> crystals [6]. An indication of this is the small RD_1 spread observed at 50% (Figure 1b) which can be compared to that in straight rolled copper after only 10% reduction [6]. Thus slip on BII, DIII is assumed to stop somewhere between 20% and 40% reduction. The reason for this lies in the special

feature of the twinned structure formed during RD_1 rolling. By twinning the crystal divides up into a layered structure of matrix-twin {112}<111> and {552}<115> lamellae which are very thin. The micrographs taken at 80% reduction (Figure 3) shows fine twins which are also representative of the 50% rolled structure. This structure provides obstacles for all slip systems except for those having the slip plane parallel to the twinning plane. In {112}<111> and {552}<115> the systems AV, AVI and AIV, AV respectively are favoured. Upon activation the matrix-twin orientations are rotated towards {111}<112>, which is observed in Figure 1c after 70% reduction. For rolling in RD_2 the favoured slip systems BII, DIII form a steep angle to the twinning plane and slip becomes increasingly difficult due to dislocation pile ups. The only unhindered systems are AIV, AV (normal slip) and A3 (partial slip) which lie parallel to the twinning planes. For these systems the Schmid factor is rather low (μ_n=0.27, μ_p=0.31) but their activation explains the widening during RD_2 rolling. Furthermore an explanation for the high volume fraction (80%) of twin orientation can be offered by assuming that the partial slip system takes most of the deformation, which is likely since μ_p/μ_n=1.15. The observation that the matrix- twin lamellae at 50% are not yet {111}<112> as they are in straight rolling can also be explained by twinning during RD_2. When twinning comes to an end and normal slip takes over in the lamellae, orientation rotation toward {111}<112> occurs. If twinning continues, however, the matrix and twin orientations stays stable in RD_2 rolling so that there is no contribution to the rotation of matrix-twin towards {111}<112> and the rotation is slow compared with straight rolled crystals. In addition to the crystal widening, its elongation can be explained by shear band formation which is more pronounced in RD_2 than RD_1 after 50%-60%.

When matrix-twin lamellae reach {111}<112> there is no slip parallel to the twinning plane nor on any other slip systems possible as discussed above. Shear banding is now the dominant deformation mechanism. The microstructure in Figure 3 show that shear bands form during both RD_1 and RD_2 rolling. From straight rolled {112}<111> crystals it is known that shear bands within the layered structure of {111}<112> yield {011}<100> which is then rotated about ND into {011}<211>[1]. In the present case the formation of {011}<100> is assumed to occur during RD_1 rolling steps, which corresponds to the straight rolled case. For RD_2 rolling the orientation path of {111}<110> toward {011}<211> is more direct, i.e. not passing through the {011}<211> orientation. This can best be visualized from the skeleton lines (Figure 2) for specimens after low reduction. For the 50% cross-rolled specimen where shear bands were detected by TEM mainly to occur during RD_2 rolling the α-fibre shows a maximum 10° off {011}<100>, and only little intensity at {011}<100>. After 70% both intensities increase, and the maximum is still the 10° shifted orientation. At 80% and 90% both components form a common peak which means that shear bands in RD_1 and RD_2 contribute the same amount to the {011}<100> and near {011}<100> peak. The clear shift of the peak toward {011}<211> and the strong decrease of {011}<100> after 95% indicates that the final rotation about ND starts only at reductions higher than 90%. This explains why the "brass-type" texture is not reached by 95%. However, it is expected that it will be reached at higher reductions and that eventually the {110}<223> cross-rolling texture

observed in polycrystalline materials of low SFE [7] will form.

ACKNOWLEDGEMENT

The authors like to thank Mr. M. J. Hua for preparing the TEM micrographs. One of the authors (HH) was supported by the National Science Foundation of the USA, Grant No. DMR-8614903. For this collaborative work in Aachen, HH was supported by the Senior Scientist Award of the Alexander von Humboldt Foundation of the FRG.

REFERENCES

[1] B.J. Duggan, M. Hatherly, W.B. Hutchinson and P.T. Wakefield , *Met.sci.*, 12, 343 (1978)

[2] K.Lücke, J.Pospiech, K.H. Virnich and J.Jura, *Acta metall.*, 29, 167 (1981)

[3] U.Schmidt and K.Lücke, *Texture cry. sol.*, 3, 85 (1979)

[4] H.Hu, R.S.Cline and S.R.Goodman, *Recristallization, Grain Growth and Textures*, ed.H. Margolin, (ASM, Metals Park, OH, 1964) p.295

[5] G.D.Köhlhoff, A.S.Malin, K.Lücke and M.Hatherly, *Acta metall.*, 36, 284 (1988) G.D.Köhlhoff, Ph.D. thesis, RWTH Aachen (1988)

[6] X.Sun, G.D.Köhlhoff and K.Lücke, to be published

[7] H.Hu and R.S.Cline, *Textures and Microstructures*, 8 & 9, 191 (1988)

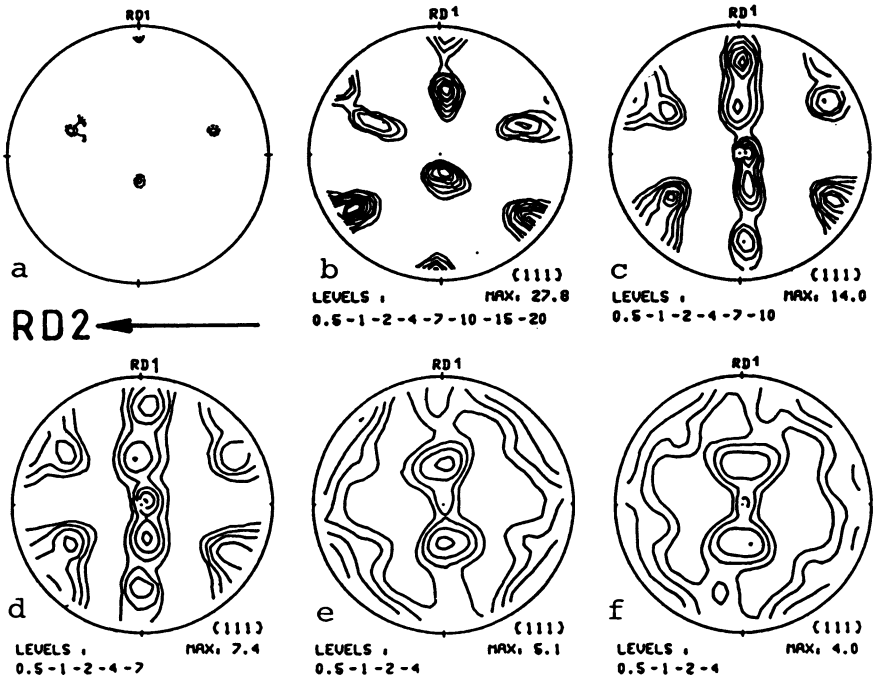

Figure 1 (111) pole figures of (a) undeformed crystal and after (b) 50%, (c) 70%, (d) 80%, (e) 90%, and (f) 95% cross rolling reduction

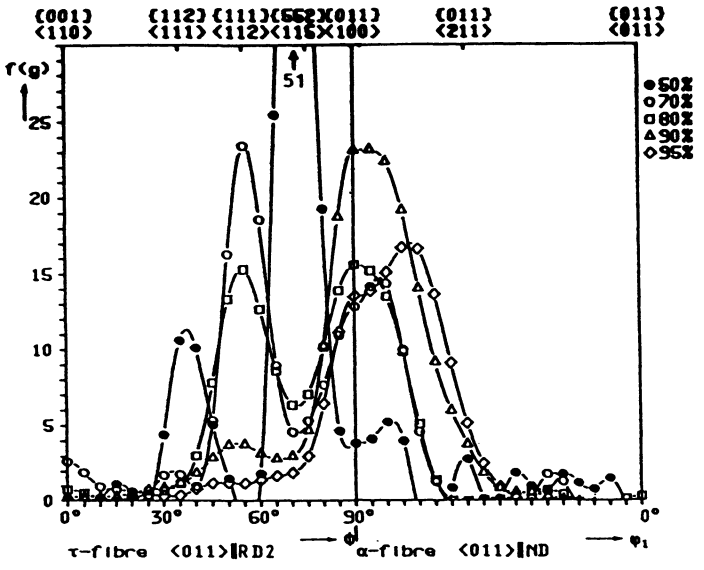

Figure 2 Skeleton lines along the τ- and α-fibre taken from ODFs

Figure 3 TEM micrograph of the 80% cross rolled specimen (longitudinal section)

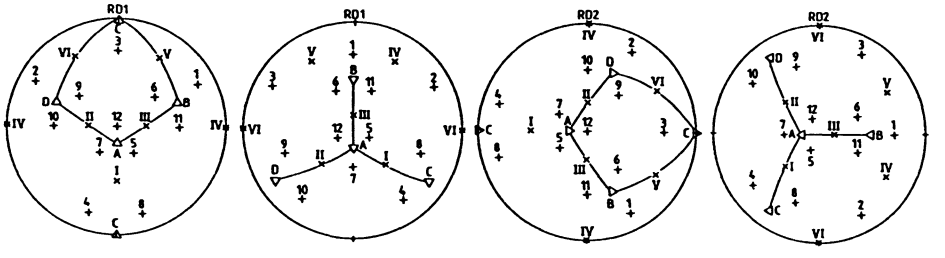

Figure 4 Stereographic projections showing slip systems of the orientations {112}<111>, {552}<115>, {112}<110>, and {552}<110>.
(Δ (111) plane normals, x <110>directions, + <112> directions)